Liver X receptors contribute to the protective immune response against *Mycobacterium tuberculosis* in mice

Hannelie Korf, … , Johan Grooten, Kris Huygen

Research Article

Liver X receptors (LXRs) are key regulators of macrophage function, controlling transcriptional programs involved in lipid homeostasis and inflammation. However, exactly how LXRs modulate inflammation during infection remains unknown. To explore this, we used a mouse model of *Mycobacterium tuberculosis* infection. Upon intratracheal infection with *M. tuberculosis*, LXRs and LXR target genes were induced in CD11c$^+$ lung and alveolar cells. Furthermore, mice deficient in both LXR isoforms, LXRα and LXRβ (*Lxra$^{-/-}$Lxrb$^{-/-}$* mice), were more susceptible to infection, developing higher bacterial burdens and an increase in the size and number of granulomatous lesions. Interestingly, mice solely deficient in LXRα, but not those lacking only LXRβ, mirrored the susceptibility of the *Lxra$^{-/-}$Lxrb$^{-/-}$* animals. *Lxra$^{-/-}$Lxrb$^{-/-}$* mice failed to mount an effective early neutrophilic airway response to infection and showed dysregulation of both pro- and antiinflammatory factors in CD11c$^+$ lung cells. T cell responses were strongly affected in *Lxra$^{-/-}$Lxrb$^{-/-}$* mice, showing near-complete abrogation of the infection-induced Th1 function — and even more so Th17 function — in the lungs. Treatment of WT mice with the LXR agonists TO901317 and GW3965 resulted in a 10-fold decrease of the pulmonary bacterial burden and a comparable increase of Th1/Th17 function in the lungs. The dependence of LXR signaling on the neutrophil IL-17 axis represents what we believe to be a novel function for these nuclear receptors in […]

Find the latest version:

https://jci.me/35288/pdf

Liver X receptors contribute to the protective immune response against *Mycobacterium tuberculosis* in mice

Hannelie Korf,[1] Seppe Vander Beken,[2] Marta Romano,[1] Knut R. Steffensen,[3] Benoît Stijlemans,[4] Jan-Åke Gustafsson,[3] Johan Grooten,[2] and Kris Huygen[1]

[1]Laboratory of Mycobacterial Immunology, Scientific Institute of Public Health, Brussels, Belgium.
[2]Laboratory of Molecular Immunology, Department of Molecular Biology, Ghent University, Ghent, Belgium.
[3]Department of Biosciences and Nutrition at Novum, Karolinska Institute, Huddinge, Sweden. [4]Laboratory of Cellular and Molecular Immunology, VIB Department of Molecular and Cellular Interactions, Vrije Universiteit Brussel, Elsene, Belgium.

Liver X receptors (LXRs) are key regulators of macrophage function, controlling transcriptional programs involved in lipid homeostasis and inflammation. However, exactly how LXRs modulate inflammation during infection remains unknown. To explore this, we used a mouse model of *Mycobacterium tuberculosis* infection. Upon intratracheal infection with *M. tuberculosis*, LXRs and LXR target genes were induced in CD11c+ lung and alveolar cells. Furthermore, mice deficient in both LXR isoforms, LXRα and LXRβ (*Lxra−/−Lxrb−/−* mice), were more susceptible to infection, developing higher bacterial burdens and an increase in the size and number of granulomatous lesions. Interestingly, mice solely deficient in LXRα, but not those lacking only LXRβ, mirrored the susceptibility of the *Lxra−/−Lxrb−/−* animals. *Lxra−/−Lxrb−/−* mice failed to mount an effective early neutrophilic airway response to infection and showed dysregulation of both pro- and antiinflammatory factors in CD11c+ lung cells. T cell responses were strongly affected in *Lxra−/−Lxrb−/−* mice, showing near-complete abrogation of the infection-induced Th1 function — and even more so Th17 function — in the lungs. Treatment of WT mice with the LXR agonists TO901317 and GW3965 resulted in a 10-fold decrease of the pulmonary bacterial burden and a comparable increase of Th1/Th17 function in the lungs. The dependence of LXR signaling on the neutrophil IL-17 axis represents what we believe to be a novel function for these nuclear receptors in resistance to *M. tuberculosis* infection and may provide a new target for therapeutics.

Introduction

An estimated one-third of the world population is latently infected with *Mycobacterium tuberculosis* (1), creating a vast reservoir from which most active cases of tuberculosis arise. The success of *M. tuberculosis* as a pathogen lies in its ability to adapt and survive for long periods of time within the host macrophage in a state of clinical dormancy (2). *M. tuberculosis* mobilizes specific transcriptional pathways when grown under conditions that mimic the microenvironment of persisting dormant bacilli in lung granulomas (3–5). Of particular interest is that the bacilli, faced with the nutrient-deficient macrophage phagosome, switch to lipids as their main carbon source (6, 7). The lipid-based metabolism is implicated in virulence and is crucial for the survival of tubercle bacilli in vivo (8, 9). Recent studies delineated an entire cluster of genes involved in lipid degradation in *M. tuberculosis* and related *Mycobacterium* spp., demonstrating the pathogen's unusually large repertoire of lipid metabolism machinery (10, 11). Interestingly, within this regulon, an extended number of genes encodes enzymes important in the uptake and catabolism of cholesterol (11). Several genes within the deduced steroid catabolic pathway

are essential for long-term survival in macrophages, thereby illustrating the critical nature of this pathway (3, 4, 11). More directly, a recent report implicated that mycobacterial persistence is critically linked to its ability to acquire and catabolize cholesterol from the host (12). Cholesterol, besides being used as an energy or carbon source, is also essential for the phagocytosis of the bacterium by the macrophage and for the inhibition of phagosome maturation (13–15). To ensure sufficient availability of the sterol, mycobacteria may have to rely on lipid import by the host macrophage. In support of this, we recently demonstrated that mycolic acid, a major mycobacterial cell wall component, strongly interfered with the lipid metabolism of macrophages, triggering intracellular accumulation of cholesterol, increased cell size, and multiple vacuole formation, all typical features of macrophage foam cells (16). Foamy macrophages constitute a characteristic trait of mycobacterial infections and a safe haven for mycobacteria, since they have been found to harbor multiple bacilli (17–19).
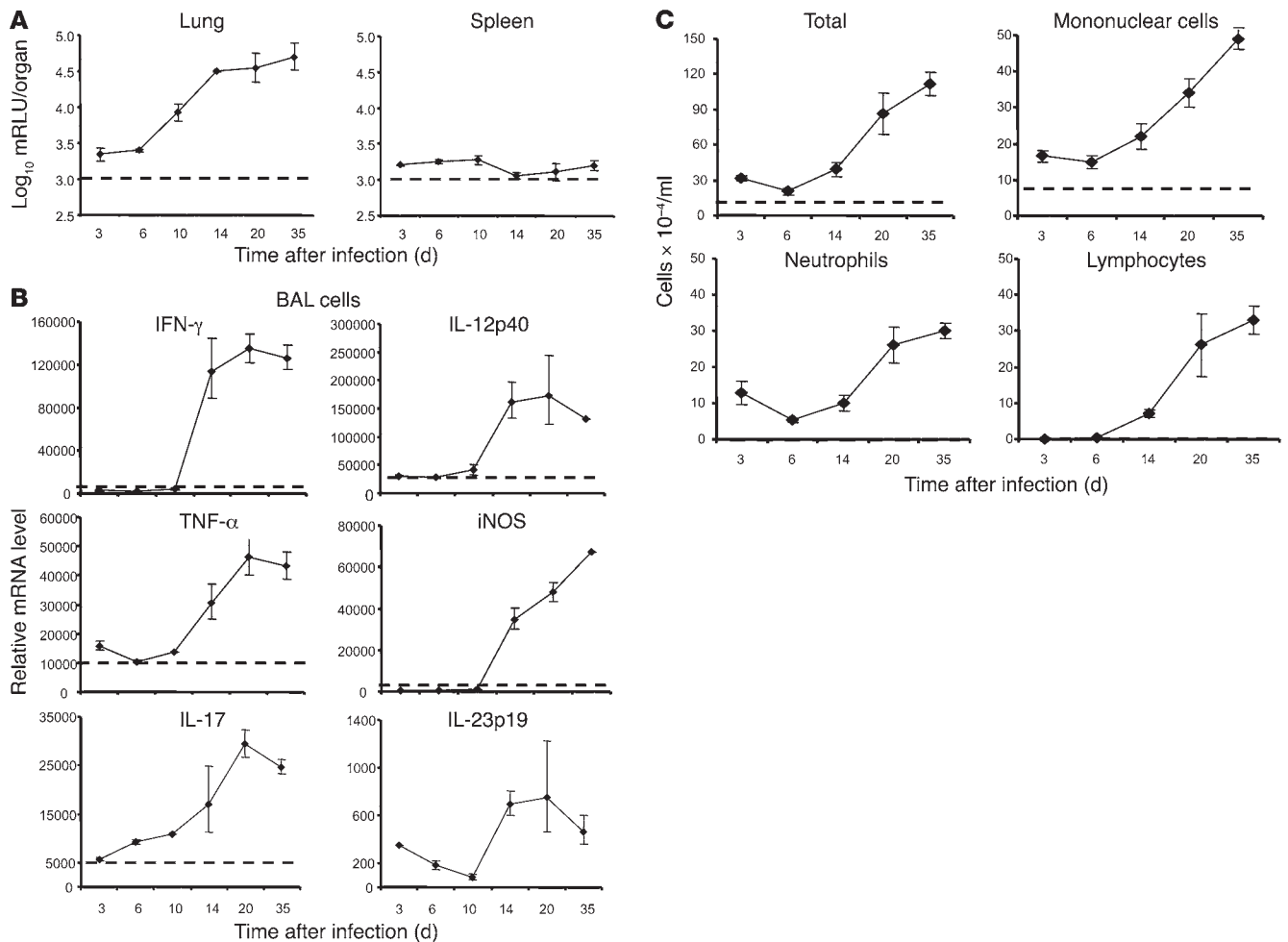
Macrophage lipid import and export mechanisms must be tightly regulated, because a disturbance of this balance can lead to metabolic disorders. Disturbed lipid homeostasis by uncontrolled lipid import also affects the inflammatory status of the macrophage. Recently, liver X receptors (LXRs), LXRα and LXRβ, have emerged as master regulators of macrophage transcriptional programs involved in cholesterol, fatty acid, and glucose homeostasis (20–22). LXRs represent a subset of the nuclear receptor superfamily that is regulated by oxidized forms of cholesterol (oxysterols) and intermediate products of the cholesterol biosynthetic pathway (23–25). The inducible LXRα is expressed highly in the liver,

Figure 1
Characteristic features of the murine pulmonary tuberculosis model. (**A**) Bacterial counts in the lungs and spleen at different time points after i.t. instillation of luminescent *M. tuberculosis* (1×10^4 CFU). Values are expressed as $\log_{10}$ mRLU per organ ($n = 4$). Dotted lines indicate the detection limit of the bioluminescence assay. (**B**) RT-qPCR analysis of the indicated inflammatory mediators within BAL cells. Data are expressed as relative mRNA levels, normalized against reference the housekeeping gene. Mice were tested individually ($n = 4$). Dotted lines denote mRNA levels obtained from background-matched naive BAL cells. (**C**) Cellular infiltration in the airways after exposure to the pathogen. Shown are absolute numbers of total cells, mononuclear cells, neutrophils, and lymphocytes. Dotted lines denote cell numbers in naive animals. Data in **C** are mean ± SEM ($n = 5$).

adrenal glands, intestine, adipose tissue, macrophages, lung, and kidney, whereas LXRβ is ubiquitously expressed (26). The ligand-activated transcription factors form obligate heterodimers with the retinoid X receptor (RXR) and regulate the expression of target genes containing LXR response elements (27). LXR activation in macrophages induces expression of several genes involved in cholesterol trafficking and efflux, including genes encoding ABCA1, ABCG1/ABCG4, and apoE (28, 29). Besides their well-established role as cholesterol sensors and regulators, LXRs also control transcriptional programs involved in the inflammatory response. In murine macrophages, LXR activation has been shown to inhibit TLR-4–mediated LPS responses by antagonizing the nuclear factor–κB pathway (30–32). Inversely, TLR-4 activation can inhibit LXR-induced cholesterol efflux from macrophages, indicating a physiological crosstalk between inflammation and lipid metabolism (33). However, activation of LXRs can also potentiate LPS-induced responses in human macrophages, implicating a positive

regulation of macrophage-mediated inflammation (34). Moreover, by their ability to inhibit pathogen-induced macrophage apoptosis, LXRs may indirectly contribute to the host innate immune response (32, 35). Owing to their ability to regulate cholesterol metabolism and inflammatory signaling, LXRs have emerged as potential targets for metabolic and inflammatory diseases (36). However, the ability of endogenous LXR-dependent pathways to modulate inflammation in infectious disease settings remains to be determined. Here we demonstrate that LXRs contributed to the protective immune response during experimental aerogenic infection with the intracellular pathogen *M. tuberculosis*. Treatment with an LXR agonist reduced bacterial replication in *M. tuberculosis*–infected mice. Inversely, *Lxra⁻/⁻Lxrb⁻/⁻* mice, deficient in both LXRα and LXRβ, exhibited increased susceptibility to infection and a concomitant defective innate and acquired immune response. Our results implicate LXR-dependent pathways in the protective immune response against this major pathogen.
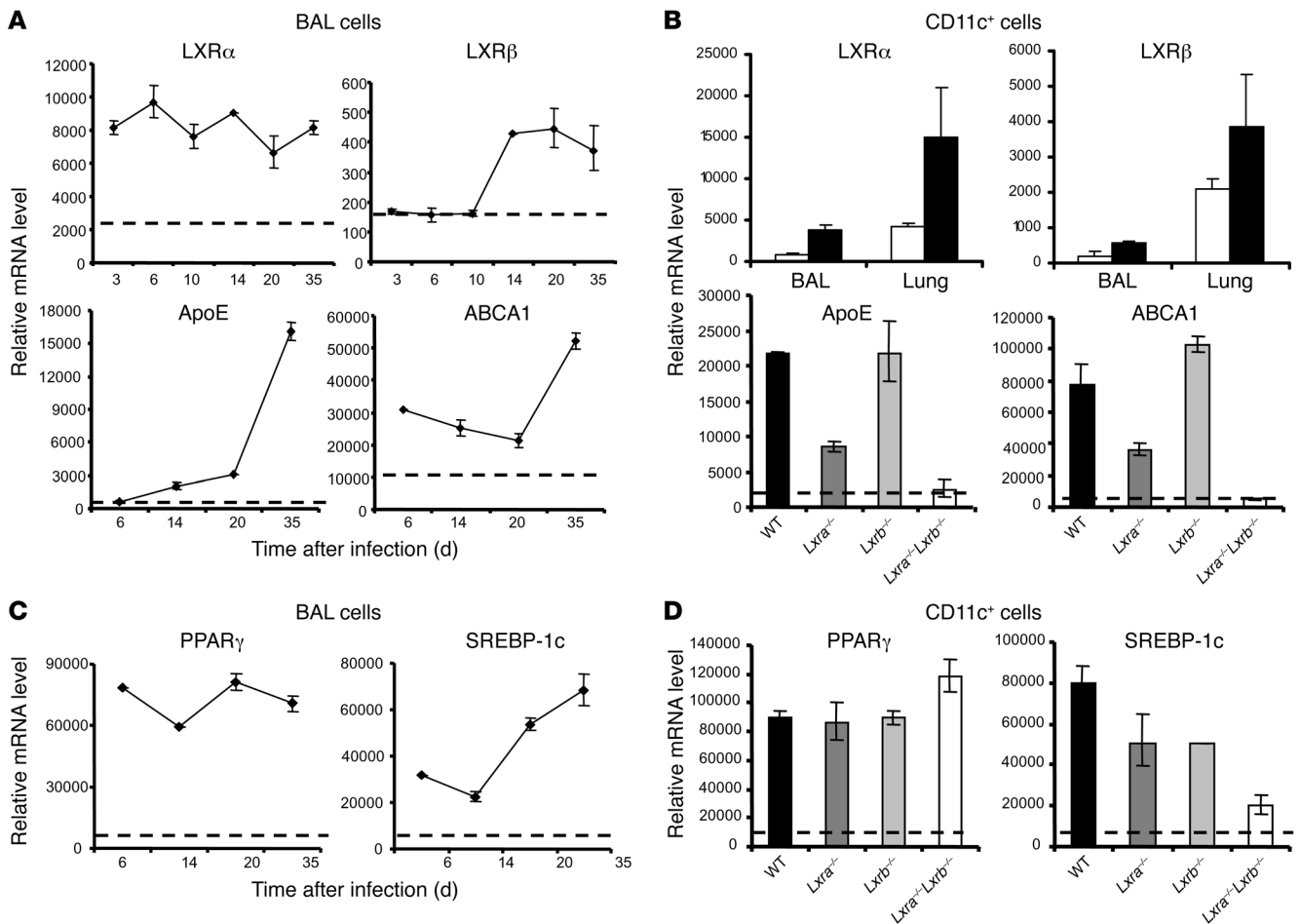
Figure 2
Expression of LXRs and LXR-dependent genes during *M. tuberculosis* infection. (**A** and **C**) RT-qPCR analysis of expression levels of LXRα and LXRβ isoforms, LXR-dependent target genes, and PPARγ and SREBP-1c within BAL cells isolated at the indicated times after infection. Dotted lines denote mRNA levels obtained from background-matched naive BAL cells. Mice were tested individually ($n = 4$–5). (**B** and **D**) After 3 weeks of infection, CD11c+ cells were isolated from the BAL, and lung tissue digests and relative mRNA levels of the indicated parameters were determined by RT-qPCR. (**B**, top) Infected (black bars) CD11c+ BAL and lung cells or naive controls (white bars) from WT mice. (**B**, bottom, and **D**) Transcriptional analysis of CD11c+ BAL cells isolated from infected WT, *Lxra*−/−, *Lxrb*−/−, and *Lxra*−/−*Lxrb*−/− mice ($n = 5$). Dotted lines denote mRNA levels obtained from background-matched naive CD11c+ BAL cells.

Results

Infection kinetics of the experimental pulmonary tuberculosis model. We used an airway infection model in which mice were instilled with $5 × 10^3$ mRLU of luminescent *M. tuberculosis* H37Rv intratracheally (i.t.) and monitored for bacillary growth at different time intervals. This inoculum corresponded to 10^4 CFU by standard plating techniques (data not shown) and established an initial load of $3 × 10^3$ mRLU in the lungs. The infection slowly progressed into an exponential growth phase (days 6–14), followed by a chronic phase, as the bacterial numbers started to stabilize at close to $5 × 10^4$ mRLU/lung (days 20–35; Figure 1A). The infection remained local during the 5 weeks of the experiment, as evidenced by minimal dissemination to the spleen (Figure 1A). Another characteristic feature of *M. tuberculosis* infection is a strong proinflammatory response triggered in the airways, keeping the bacterial growth in check. Increased mRNA levels of typical inflammatory mediators IFN-γ, TNF-α, IL-12p40, and iNOS were observed from day 14 after infection, corresponding to the bacterial growth arrest initiating

the chronic phase (Figure 1B). After day 20, expression levels were either sustained or decreased slightly. Expression of IFN-γ in particular was triggered strongly by *M. tuberculosis* infection, as reflected by cytokine concentrations in the BAL fluid of up to 800 pg/ml on day 14 after infection (data not shown). Similar results were obtained with transcriptional analysis of these parameters in lung tissue (data not shown). Interestingly, increased mRNA levels of IL-17 and IL-23p19 were also observed after airway challenge with the pathogen (Figure 1B), thus underscoring the mixed Th1/Th17 nature of the cytokine function in the airways of this experimental model. In line with these findings, the cellular composition of the airway response to *M. tuberculosis* infection featured early infiltration of neutrophils and mononuclear cells. These 2 cell populations steadily increased during the course of the infection, mononuclear cells always representing the majority of the cells present in the airway lumen. Lymphocytes became apparent only at day 14 after the initial pathogen encounter and increased until day 20 (Figure 1C).
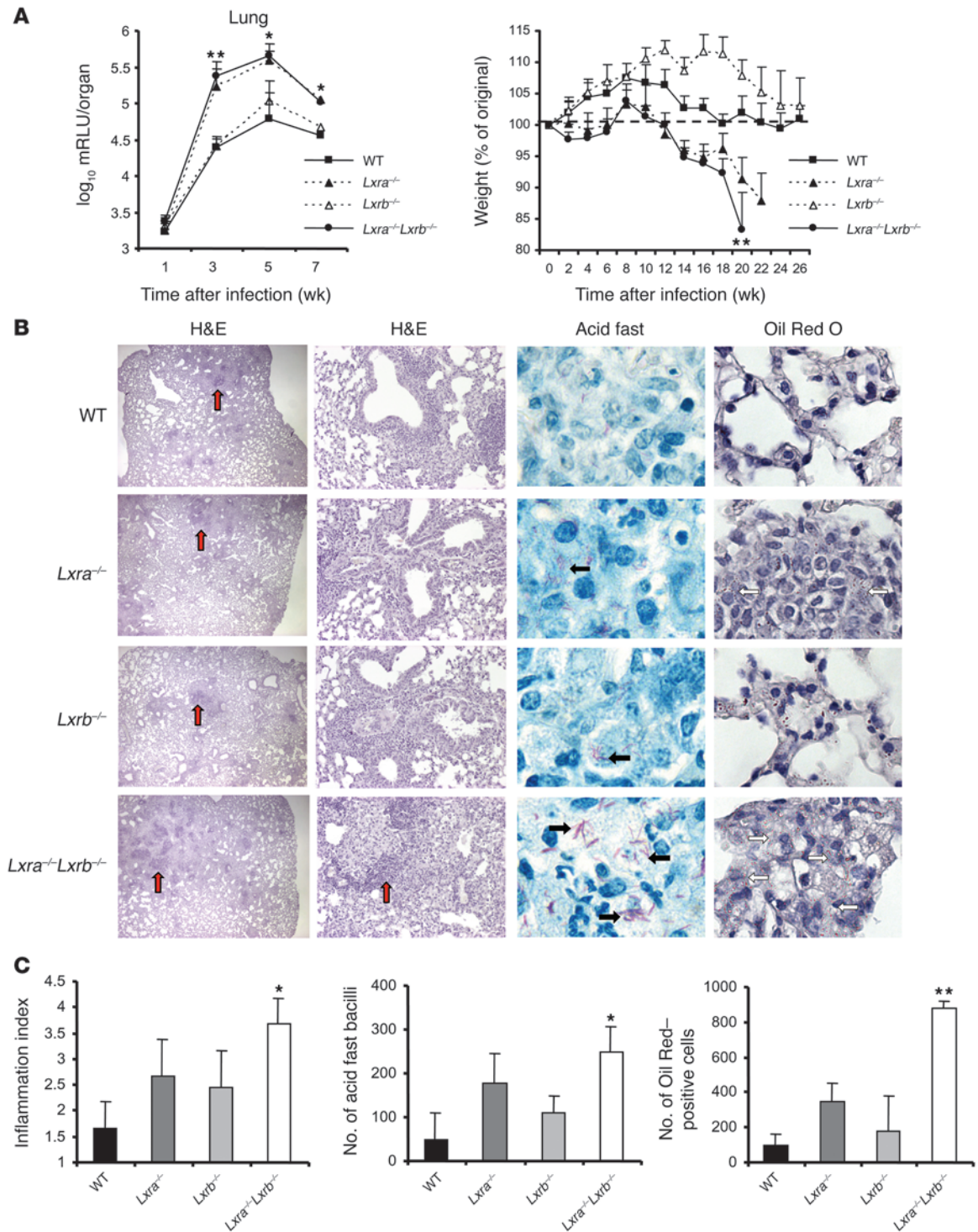
Figure 3
Mice lacking LXRs are more susceptible to *M. tuberculosis* infection. (**A**) Changes in bacterial load in the lungs and total body mass of WT, *Lxra*⁻/⁻, *Lxrb*⁻/⁻, and *Lxra*⁻/⁻*Lxrb*⁻/⁻ mice infected i.t. with *M. tuberculosis* (1×10^4 CFU). Values are expressed as $\log_{10}$ mRLU per organ and as percent of original weight (n = 5–7). *$P < 0.05$, **$P < 0.01$, *Lxra*⁻/⁻*Lxrb*⁻/⁻ versus WT. (**B**) Histological analysis of H&E-stained lungs sections at 5 weeks after infection revealed more extensive granulomatous inflammation (red arrows) as well as total inflammation in the in *Lxra*⁻/⁻*Lxrb*⁻/⁻ mice. Acid fast staining of the sections showed the presence of mycobacteria as pink rods. Frequent events of multiple bacteria per cell were observed in the lung sections from *Lxra*⁻/⁻ and *Lxra*⁻/⁻*Lxrb*⁻/⁻ mice (black arrows). Foamy macrophages containing multiple red lipid droplets after staining with Oil Red O was most prominent in *Lxra*⁻/⁻ and *Lxra*⁻/⁻*Lxrb*⁻/⁻ mice (white arrows). Original magnification (left to right), ×20, ×100, ×1,000, ×600. (**C**) Quantification of the lung inflammation index, number of bacilli, and Oil Red–positive cells, as described in Methods (n = 5). *$P < 0.05$, **$P < 0.01$ versus WT.
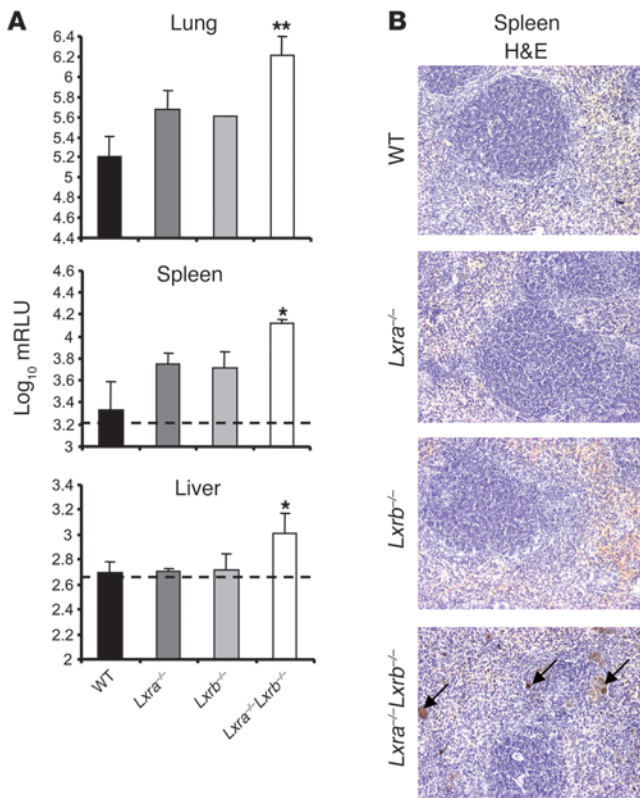
Figure 4
Infection of *Lxra⁻/⁻Lxrb⁻/⁻* mice results in disseminated systemic infection. (**A**) Bacterial load in the lungs, spleens, and livers of WT, *Lxra⁻/⁻*, *Lxrb⁻/⁻*, and *Lxra⁻/⁻Lxrb⁻/⁻* mice infected i.t. with luminescent *M. tuberculosis* (1×10^5 CFU) for 5 weeks. Values are expressed as $\log_{10}$ mRLU per organ ($n = 3$). Dotted lines indicate the detection limit of the bioluminescence assay. *$P < 0.05$, **$P < 0.01$ versus WT. (**B**) Histological analysis of spleen sections prepared after 5 weeks of infection revealed the presence in *Lxra⁻/⁻Lxrb⁻/⁻* mice of multiple macrophages with a brown reaction product after standard H&E staining (arrows). Original magnification, ×100.

LXRs and LXR target genes are induced in response to airway infection with M. tuberculosis. To investigate a possible role for LXR-dependent pathways during *M. tuberculosis* infection, we assessed the expression levels of LXRs and LXR target genes in the total cell population isolated from the bronchoalveolar lumen. LXRα mRNA was induced as early as 3 days after infection, and remained high (despite fluctuating) at all time points tested (Figure 2A). In contrast, expression levels of LXRβ were in general much lower than those observed for LXRα and remained basal for the first 10 days after infection, after which a moderate increase was observed (Figure 2A). Because increased expression cannot always be correlated to functional activity of LXR (33), we evaluated relative mRNA levels of well-documented LXR target genes — cholesterol transporter, ABCA1, and ApoE — as readout for LXR activation. Markedly increased expression levels in BAL cells for both LXR target genes were observed throughout the course of infection (Figure 2A). Analysis of the CD11c⁺ cell fraction from the BAL, as well as analysis of lung tissue, at day 21 after infection confirmed this assessment, showing strong induction of LXRα in contrast to moderate induction of LXRβ (Figure 2B). The CD11c⁺ population was selected because it contains the majority of macrophages together with some DCs (37) and represents the cellular target of *M. tuberculosis*. Additionally, mRNA levels for ApoE and ABCA1 markedly increased as a result of *M. tuberculosis* infection (Figure 2B). The dependence on LXR transcriptional activity of the infection-induced increment was confirmed by the partial to complete abolishment of induction with single-knockout *Lxra⁻/⁻* and double-knockout *Lxra⁻/⁻Lxrb⁻/⁻* mice, respectively (Figure 2B).

Besides LXRs, airway challenge with *M. tuberculosis* also triggered the expression of PPARγ and SREBP-1c, additional transcription factors prominent in the regulation of lipid metabolism pathways. Increased mRNA levels of these transcription factors were observed in cells from the BAL at different time points after infection and, similar to the results for LXRα, were highly induced in CD11c⁺ cells from the airway lumen (Figure 2, C and D). However, LXR deficiency did not alter the expression levels of PPARγ, a nuclear receptor upstream of LXRα. On the other hand, loss of both LXR isoforms did result in a pronounced reduction in the relative mRNA levels of SREBP-1c, which is by itself a known LXR target (Figure 2D). These results demonstrate prominent activation of LXRs and their downstream pathways during infection with *M. tuberculosis*, implicating a possible role for them in the host response.

Mice lacking LXRs are more susceptible to M. tuberculosis infection. We verified the involvement of LXRs during experimental pulmonary tuberculosis by challenging *Lxra⁻/⁻Lxrb⁻/⁻* mice with *M. tuberculosis* using the same model described above. Whereas WT mice effectively stabilized bacillary growth in the lungs at around 5×10^4 mRLU, the bacterial burden in the lungs of background-matched *Lxra⁻/⁻Lxrb⁻/⁻* mice was approximately 10-fold higher after 3 weeks of infection (Figure 3A). Susceptibility to *M. tuberculosis* infection was associated primarily with the loss of LXRα and not LXRβ, since the bacterial load in the lungs of *Lxra⁻/⁻* mice was almost identical to that of *Lxra⁻/⁻Lxrb⁻/⁻* mice, while bacterial replication in *Lxrb⁻/⁻* mice was not different from that in WT animals. In line with these results, only *Lxra⁻/⁻* mice and *Lxra⁻/⁻Lxrb⁻/⁻* mice showed accelerated cachexia 14–20 weeks after infection (Figure 3A). After 21 weeks, *Lxra⁻/⁻Lxrb⁻/⁻* mice reached a point at which they had to be euthanized, having lost more than 20% of their initial body weights. Previous experiments demonstrated that background-matched animals survive up to a year without any physical sign of disease with this i.t. infection dose (our unpublished observations). Histological analysis at 5 weeks of infection revealed a marked increase in the size and number of granulomatous lesions that was most pronounced in *Lxra⁻/⁻Lxrb⁻/⁻* mice (Figure 3, B and C). Moreover, a high percentage of lesions in *Lxra⁻/⁻Lxrb⁻/⁻* as well as *Lxra⁻/⁻* mice contained numerous acid fast bacteria within foamy macrophages and showed multiple lipid-loaded cells, as demonstrated by Oil Red O staining of the lung tissue sections (Figure 3, B and C).

Airway infection models mimic human pulmonary tuberculosis in the sense that the bacilli remain locally in the lungs with minimal dissemination to other organs, as we observed in Figure 1A. In order to verify whether *Lxra⁻/⁻Lxrb⁻/⁻* mice are able to restrict infection to the pulmonary cavity, we challenged the airways with a 10-fold higher inoculum (10^5 CFU) of luminescent *M. tuberculosis* and analyzed the bacterial burden in lungs, spleen, and liver after 5 weeks of infection. The data obtained confirmed the previous result, showing increased bacterial load in the lungs of *Lxra⁻/⁻Lxrb⁻/⁻* mice compared with WT animals. In addition, *Lxra⁻/⁻Lxrb⁻/⁻* mice failed to contain the infection: significant levels of bacteria were detected in the spleen (Figure 4A). Interestingly,
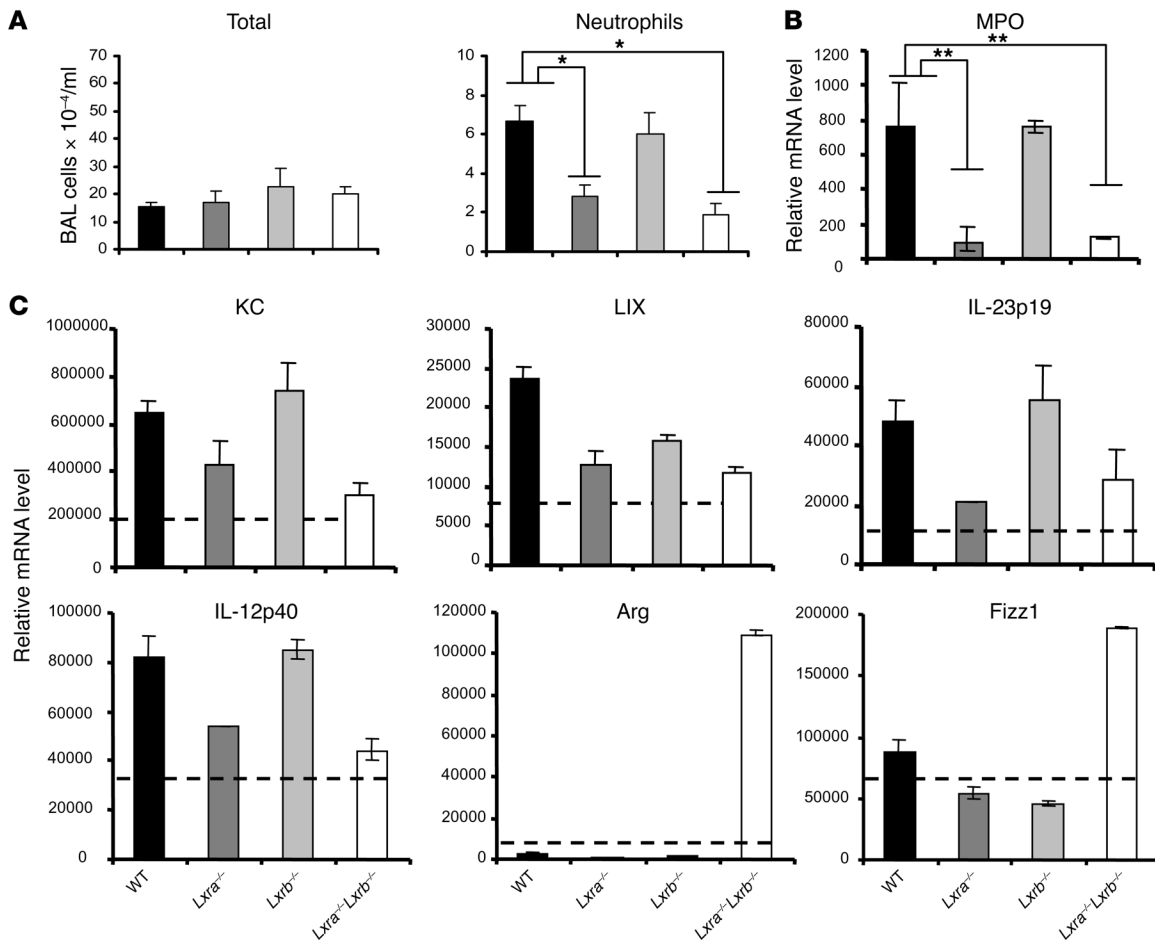
Figure 5
LXR-dependent regulation of the innate immune response after i.t. challenge with *M. tuberculosis*. WT, *Lxra*−/−, *Lxrb*−/−, and *Lxra*−/−*Lxrb*−/− mice were infected i.t. with luminescent *M. tuberculosis* (1 × 10⁴ CFU) and sacrificed 7 days after infection. (**A**) Differential cell infiltration in the BAL. Shown are the absolute numbers of total cells and neutrophils. Data in **A** are mean ± SEM (*n* = 5). (**B**) Relative mRNA levels of MPO from total lung tissue samples, as determined by RT-qPCR (*n* = 5). (**C**) CD11c⁺ cells were isolated 7 days after infection from lung tissue digests, and relative mRNA levels were determined by RT-qPCR. Dotted lines denote values obtained from CD11c⁺ cells of naive mice. Data are expressed as relative mRNA levels, normalized against reference housekeeping genes (*n* = 5), and are representative of 2 separate experiments. Arg, arginase. *$P < 0.05$, **$P < 0.01$.

histological analysis of spleen sections by standard H&E staining revealed numerous macrophages from *Lxra*−/−*Lxrb*−/− mice containing lipofuscin-like particles (Figure 4B). This could be indicative of an overload of lipid oxidation products that interact with cell proteins and lead to the formation of yellow-brown oxidized protein aggregates. Alternatively, these particles could be indicative of increased phagocytosis of red blood cells, resulting in the accumulation of hemosiderin as the brown iron-containing catabolic product. In the liver, in which bacterial replication after i.t. infection with *M. tuberculosis* was tightly controlled in WT mice, bacterial numbers from *Lxra*−/−*Lxrb*−/− mice were clearly above the basal level (Figure 4A). These data support a crucial role for LXR-dependent pathways, and especially for LXRα, in the control and containment of infection with *M. tuberculosis*.

LXRs regulate the innate response to M. tuberculosis infection. Mycobacterial infection typically results in the induction of a local inflammatory response that culminates in granuloma formation. As documented above, this response, initiated shortly after

the bacterium-macrophage interaction, was characterized by the recruitment of innate effector cells, such as macrophages, polymorphonuclear neutrophils, and NK cells, to the infectious foci. To verify whether the increased susceptibility of the *Lxra*−/−*Lxrb*−/− mice could be linked to a defective innate response, we analyzed the acute (day 7) airway inflammatory response to pulmonary *M. tuberculosis* infection. *Lxra*−/− and *Lxra*−/−*Lxrb*−/− mice failed to mount an effective neutrophilic inflammatory response, as demonstrated by the minimal neutrophil cell numbers in the BAL compared with WT mice (Figure 5A). The number of total as well as mononuclear cells from the airway lumen remained stable in all the groups tested, while lymphocyte counts were marginal (data not shown). Real-time quantitative PCR (RT-qPCR) analysis of myeloperoxidase (MPO), a marker for activated neutrophils (38), confirmed the defective neutrophilic inflammation in *Lxra*−/−*Lxrb*−/− and *Lxra*−/− mice 7 days after infection, showing only basal mRNA levels in the lung tissue (Figure 5B). Furthermore, CD11c⁺ lung cells from
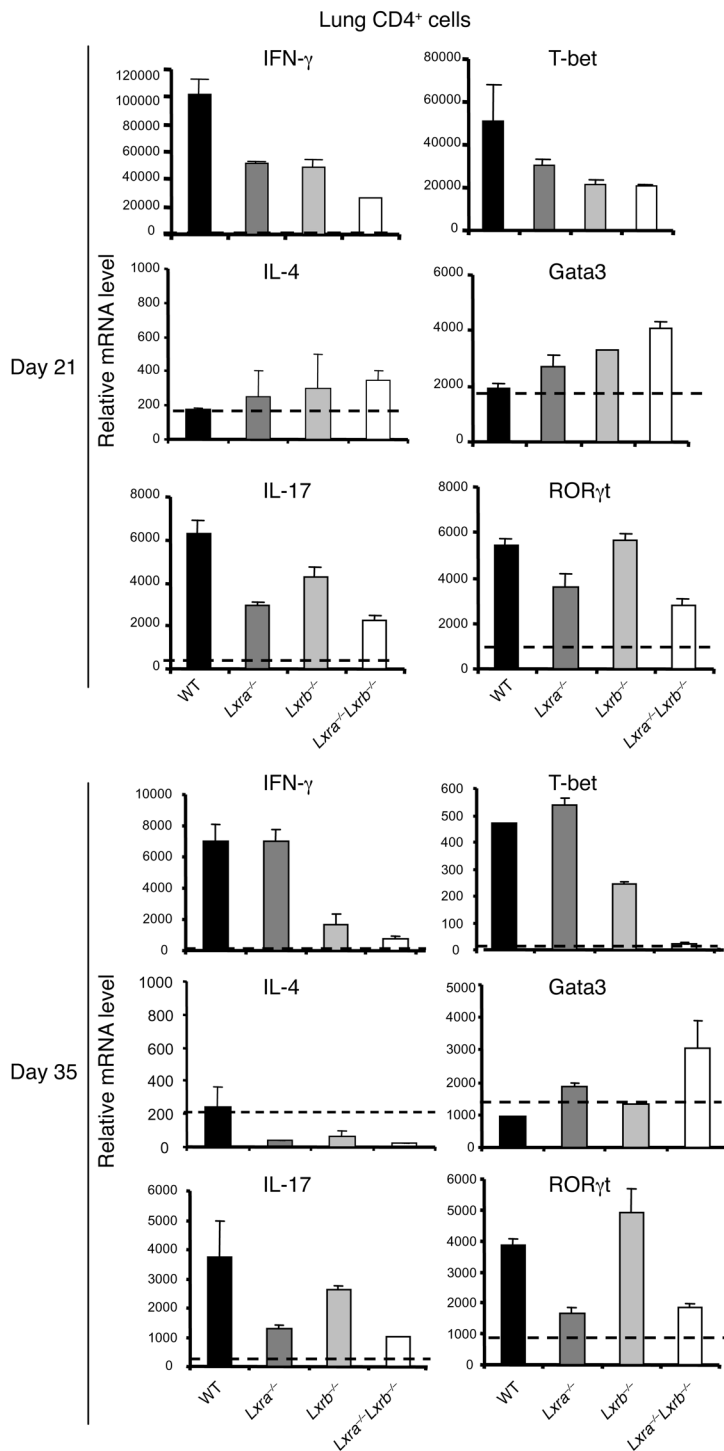
Lung CD4⁺ cells

Figure 6
The role of LXRs in the modulation of T cell function during *M. tuberculosis* infection. WT, *Lxra⁻/⁻*, *Lxrb⁻/⁻*, and *Lxra⁻/⁻Lxrb⁻/⁻* mice were infected i.t. with luminescent *M. tuberculosis* (1 × 10⁴ CFU). After 21 and 35 days of infection, CD4⁺ lung T cells were isolated, and the relative mRNA levels of Th1 (IFN-γ and T-bet), Th2 (IL-4 and Gata3), and Th17 (IL-17 and RORγt) markers were analyzed by RT-qPCR. Data are expressed as relative mRNA levels, normalized against reference housekeeping genes (*n* = 5). Results are representative of 2 separate experiments.

Finally, mRNA levels of the characteristic inflammatory mediators iNOS and TNF-α were still at basal levels in isolated CD11c⁺ lung cells of both WT and LXR-deficient animals after 7 days of infection (data not shown). However, IL-12p40 was induced at this early time point in CD11c⁺ cells from WT animals, but showed no induction or was induced only marginally in CD11c⁺ cells from *Lxra⁻/⁻* and *Lxra⁻/⁻Lxrb⁻/⁻* mice (Figure 5C). In contrast to this apparent reduction in the IL-12/IL-23 inflammatory axis, mRNA levels of arginase and found in inflammatory zone–1 (Fizz1), both prominent IL-4– and IL-13–dependent anti-inflammatory macrophage markers (40–43), were highly increased in CD11c⁺ lung cells from *Lxra⁻/⁻Lxrb⁻/⁻* mice (Figure 5C). Interestingly, expression of these markers has previously been shown to be detrimental in the context of *M. tuberculosis* infection (44). These results indicate that not only may failure to raise neutrophilic effector functions contribute to the increased susceptibility of *Lxra⁻/⁻Lxrb⁻/⁻* mice observed in this study, but modulation of macrophage activation may also be a contributing factor.

Decreased Th1 and Th17 function in the lungs of Lxra⁻/⁻Lxrb⁻/⁻ mice. We also analyzed the CD4⁺ T cell response in the lungs at days 21 and 35 after infection — at which time bacterial numbers start to stabilize and the chronic phase develops. The isolated CD4⁺ T cells were not further stimulated ex vivo, and therefore represent the in vivo status of the lung CD4⁺ T cell subset. Importantly, we did not observe any difference in the number of CD4⁺ lung T cells recruited to the lungs after infection among the experimental groups (data not shown). RT-qPCR analysis of normalized numbers of T cells showed a strong inhibition of the type 1 cytokine IFN-γ and of the Th1-specific transcription factor T-bet in *Lxra⁻/⁻Lxrb⁻/⁻* mice (Figure 6). Levels of the type 2 cytokine IL-4 and the Th2-specific transcription factor Gata3 remained basal in WT mice, and only Gata3 mRNA levels increased in *Lxra⁻/⁻Lxrb⁻/⁻* mice, especially at day 35 (Figure 6). Expression of immunoregulatory cytokines IL-10 and TGF-β and of regulatory T cell markers FoxP3 and GITR was unchanged compared with infected WT animals (data not shown). However, similar to the results for IFN-γ, CD4⁺ lung T cells from *Lxra⁻/⁻Lxrb⁻/⁻* mice featured low mRNA levels of IL-17 and the Th17-specific transcription factor retinoic acid receptor–related orphan receptor–γt (RORγt) at both time points tested (Figure 6). Interestingly, *Lxra⁻/⁻* mice closely mimicked the reduced Th1 and Th17 immune function in the lungs of *Lxra⁻/⁻Lxrb⁻/⁻* mice at day 21, when the host immune defense started to stabilize bacterial expansion. However, at day 35, when the infection had become

Lxra⁻/⁻Lxrb⁻/⁻ mice expressed lower mRNA levels of the neutrophil-attracting chemokines keratinocyte-derived chemokine (KC) and LPS-induced chemokine (LIX) as well as of IL-23, a cytokine implicated in the regulation of granulopoiesis and the prevalence of IL-17–producing cells (39), compared with cells from WT mice (Figure 5C). In agreement with our bacillary growth findings, CD11c⁺ lung cells from *Lxra⁻/⁻* mice, but not *Lxrb⁻/⁻* mice, mimicked the blunted neutrophil-attracting chemokine and cytokine response observed in the *Lxra⁻/⁻Lxrb⁻/⁻* mice.
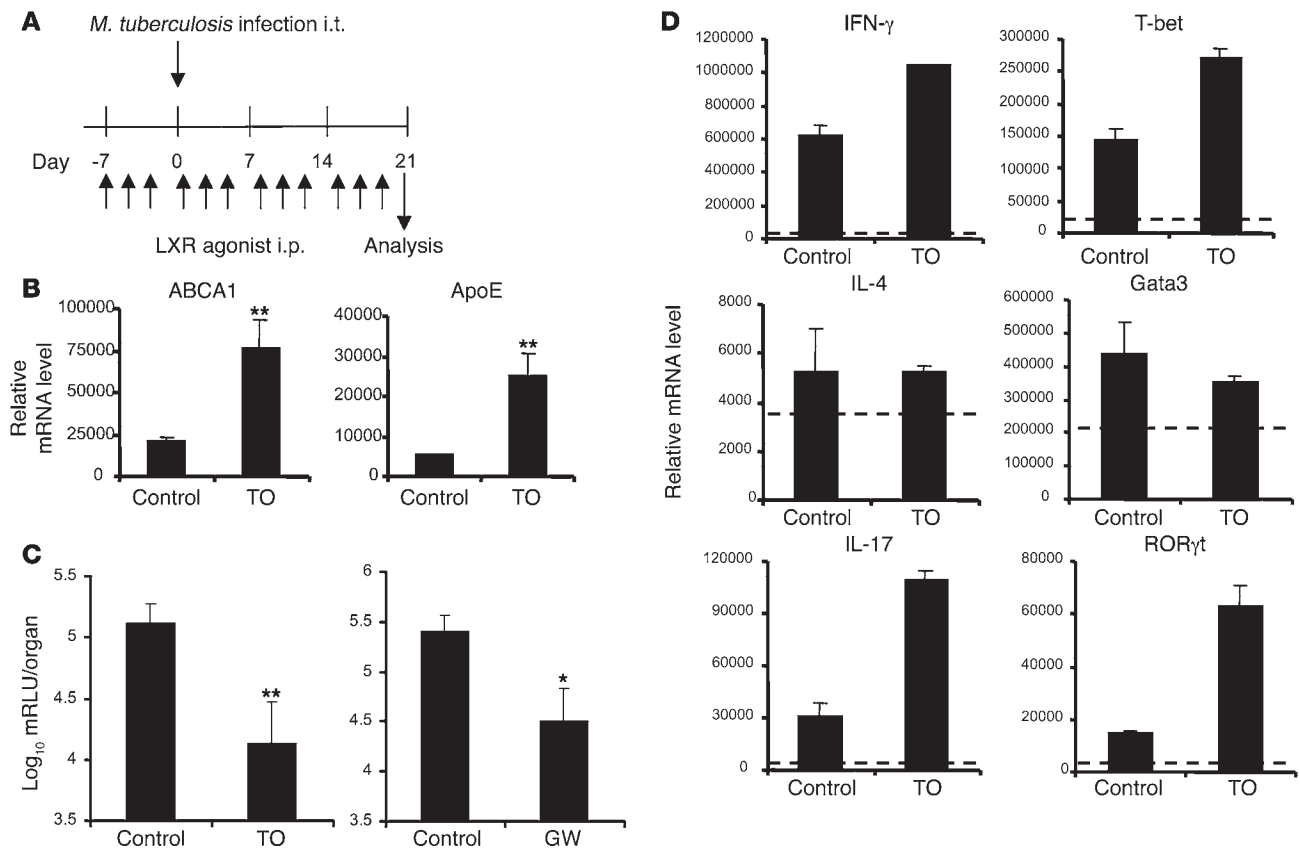
Figure 7
Prophylactic LXR agonist treatment protects mice against airway challenge with *M. tuberculosis*. (**A**) Schedule of prophylactic treatment with LXR agonist TO91317 (TO) or GW3965 (GW) in conjunction with the i.t. *M. tuberculosis* challenge model. WT C57BL/6 mice were injected i.p. 3 times per week with 50 μg agonist. (**B**) RT-qPCR analysis of LXR-dependent target gene mRNA in total BAL cells from mock-infected animals using the same treatment schedule. (**C**) Bacterial load in the lungs of treated and control groups at day 21 after infection. No difference was observed in the vehicle-treated control group and the placebo-treated group (not shown). Values are expressed as log₁₀ mRLU per organ ($n = 5$). (**D**) CD4+ lung T cells were isolated after 21 days of infection, and the relative mRNA levels of Th1, Th2, and Th17 markers (described in Figure 6) were analyzed by RT-qPCR. Data are expressed as relative mRNA levels, normalized against reference housekeeping genes ($n = 5$). Results are representative of 2 separate experiments. *$P < 0.05$, **$P < 0.01$ versus control.

chronic, IFN-γ and T-bet expression levels in *Lxra*⁻/⁻ mice were restored to normal, leaving a defective Th17 response as the most prominent feature shared between the more susceptible *Lxra*⁻/⁻ and *Lxra*⁻/⁻*Lxrb*⁻/⁻ mouse strains (Figure 6).

Treatment with LXR agonist increases resistance to M. tuberculosis infection. To address the consequences of further LXR signaling pathway activation on susceptibility to *M. tuberculosis* infection, we administered the LXR agonist TO91317 to WT mice. Treatment consisted of i.p. injection of C57BL/6 mice with 50 μg TO91317 3 times a week for 4 weeks. In a prophylactic protocol, treatment started 1 week before i.t. instillation of the bacteria. Bacillary growth in the lungs was monitored after 3 weeks of infection (Figure 7A). In a control experiment, the efficacy of the agonist in triggering the expression of the LXR target genes ABCA1 and ApoE was confirmed in mock-infected mice following the same treatment schedule (Figure 7B). Upon challenge of TO91317-treated mice with live *M. tuberculosis*, a pronounced 10-fold reduction in bacterial numbers in the lungs was observed compared with the control group (Figure 7C). Treatment with the highly LXR-specific agonist GW3965 similarly increased resistance of the mice to infec-

tion with *M. tuberculosis* (Figure 7C). In line with previous results, this further activation of LXR activity resulted in increased Th1 and Th17 responses, as evidenced by the increased mRNA levels of IFN-γ and T-bet — and even more so of IL-17 and RORγt — in CD4+ lung T cells from agonist-treated mice (Figure 7D). The mRNA expression levels of IL-4 and Gata3 remained largely unchanged.

Therapeutic postinfection treatment with the LXR agonist, in which we allowed the infection to establish for a period of 14 days before initiating a 3-week treatment (Figure 8A), produced a significant drop in bacterial load in the lungs (Figure 8, A and B). In order to verify that treatment with the LXR agonist was also capable of repressing a long-term, persistent pulmonary infection, mice were instilled i.t. with low-dose *M. tuberculosis* (1×10^2 CFU), and the infection was allowed to establish itself for 8 months before starting agonist treatment (Figure 8C). In this model of persisting tuberculosis, the 4-week treatment schedule reduced the bacterial burden in the lungs approximately 10-fold compared with control-treated animals (Figure 8D). These results highlight the importance of LXR-dependent pathways in the protective immune response both at the onset of and during further propagation of *M. tuberculosis* infection.
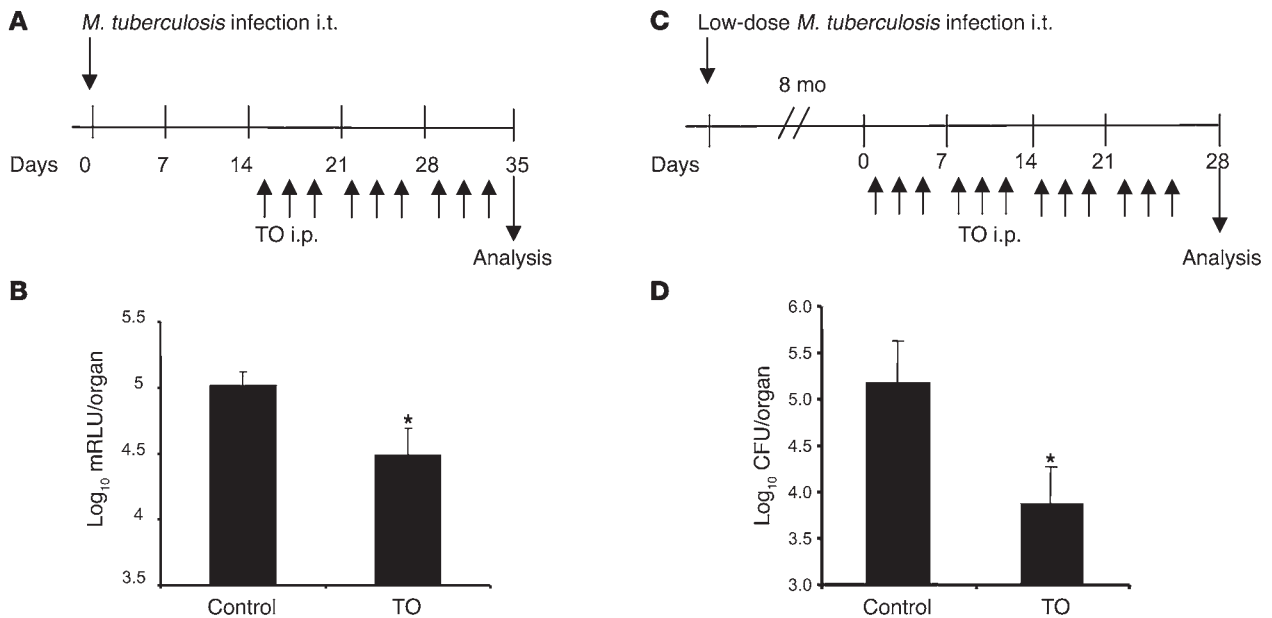
Figure 8
Therapeutic treatment with LXR agonist protects mice against airway challenge with *M. tuberculosis*. (**A** and **C**) Schedule of therapeutic treatment with TO91317 in conjunction with the i.t. *M. tuberculosis* challenge model. WT C57BL/6 mice were injected i.p. 3 times per week with 50 μg TO91317. (**B**) Bacterial load in the lungs at 35 days after infection. Values are expressed as $\log_{10}$ mRLU per organ ($n = 5$). (**D**) Bacterial load in the lungs at 28 days after infection. Values are expressed as $\log_{10}$ CFU per organ ($n = 5$). *$P < 0.05$, **$P < 0.01$ versus control.

Discussion

We have shown here that interfering with endogenous LXR signaling as master regulators of cellular and whole-body cholesterol homeostasis severely compromised the immune defense against *M. tuberculosis*, rendering the host more susceptible to the infection. *Lxra*−/−*Lxrb*−/− mice featured considerably higher bacterial burdens along with exacerbated lung pathology and progressed more rapidly to systemic infection than did WT animals after i.t. instillation of *M. tuberculosis*. Our findings suggest that a defective early neutrophilic inflammatory response, along with decreased Th17/Th1 function in the lungs, contribute to this phenotype. This notion was further confirmed in WT mice using a synthetic LXR agonist, in which increased resistance to infection as a result of further activation of LXR-signaling pathways was accompanied by increased Th17/Th1 function in the lungs. Increased resistance to infection was observed in both prophylactic and therapeutic treatment schedules, corroborating the importance of LXR signaling in the immune defense against *M. tuberculosis* once the infection is established.

The role of LXRs in infectious diseases is not fully understood and is mainly based on studies demonstrating that synthetic LXR agonists modulate macrophage responses to bacterial infection or TLR-4 engagement, thus suggesting that in addition to their role in cholesterol homeostasis, LXRs also contribute to the regulation of innate immune responses (30–32). Our data showing a crucial role for LXRs in the regulation of neutrophil- as well as macrophage-mediated inflammation strongly support this concept and highlight the role of LXRs in the control of mycobacterial infection. Interestingly, we found that the increased susceptibility of *Lxra*−/−*Lxrb*−/− mice to i.t. *M. tuberculosis* infection was primarily caused by the loss of the LXRα isoform. LXRα was highly induced in CD11c+ alveolar and lung phagocytes, the primary

cellular targets of *M. tuberculosis*, which suggests a crucial role for this isoform in the susceptible phenotype observed in the *Lxra*−/−*Lxrb*−/− animals. *Lxra*−/− mice also mimicked the abrogated airway neutrophilia observed in *Lxra*−/−*Lxrb*−/− mice early after infection. This was further reflected by the function of CD11c+ lung cells, showing a defective capacity to express the neutrophil-attracting chemokines KC and LIX as well as IL-23p19, a known regulator of granulopoiesis and instructive cytokine for IL-17–producing T cells (39). The role of neutrophils early in mycobacterial infections remains a subject of controversy. One report demonstrated an increased bacterial burden in infected organs when neutrophils are depleted at an early stage of the disease (45). However, another report failed to detect any difference in bacterial counts in neutrophil-depleted mice (46). The dysfunctional neutrophilic response and accompanying increased susceptibility to infection observed in the present study suggest that neutrophils are an essential part of the early innate defense to inhaled *M. tuberculosis*. In addition to their bactericidal effector function, neutrophils are also sources of immunoregulatory cytokines and chemokines. Accordingly, the loss of both LXR isoforms also strongly affected the nature of the subsequent T cell response, leading to near-complete abrogation of the infection-induced increment in Th1 and Th17 function in the lungs. Susceptible *Lxra*−/− mice featured a similar deficit in Th17 function, but showed only partially inhibited Th1 function, during the active growth phase of the infection at day 21. Strikingly, in WT mice treated with a synthetic LXR agonist, moderately increased Th1 immune reactivity along with a pronounced increment of Th17 reactivity accompanied the increased resistance to *M. tuberculosis*. Both results point toward a combinational role for IL-17 and (active growth phase) IFN-γ production in protective immunity against *M. tuberculosis*. IL-17, although implicated in the recruitment of neutrophils as innate

Table 1
Primers used for RT-qPCR analysis

Primer	Sequence
Gata3 forward	5′-GGCAGAAAGCAAAATGTTTGCT-3′
Gata3 reverse	5′-TGAGTCTGAATGGCTTATTCACAAT-3′
Il4 forward	5′-CCATGCTTGAAGAAGAACTCTAGTGTT-3′
Il4 reverse	5′-GACTCATTCATGGTGCAGCTTATC-3′
T-bet forward	5′-CCTACCAGAACGCAGAGATCACT-3′
T-bet reverse	5′-CACTCGTATCAACAGATGCGTACAT-3′
Ifng forward	5′-GCCAAGCGGCTGACTGA-3′
Ifng reverse	5′-TCAGTGAAGTAAAGGTACAAGCTACAATCT-3′
Rorc forward	5′-CCCCCTGCCCAGAAACACT-3′
Rorc reverse	5′-GGTAGCCCAGGACAGCACAC-3′
Il17a forward	5′-CCACGTCACCCTGGACTCTC-3′
Il17a reverse	5′-CTCCGCATTGACACAGCG-3′
Fizz1 forward	5′-CTGCTGCCAACTGTCCTAAGAAT-3′
Fizz1 reverse	5′-GGCACATGAGTCAGATTTCCAAA-3′
Arg1 forward	5′-TGAACACGGCAGTGGCTTTA-3′
Arg1 reverse	5′-GCATTCACAGTCACTTAGGTGGTTTA-3′
iNOS forward	5′-GGAGCAGGTGGAAGACTATTTCTT-3′
iNOS reverse	5′-CATGATAACGTTTCTGGCTCTTGA-3′
Tnfa forward	5′-CATCTTCTCAAAATTCGAGTGACAA-3′
Tnfa reverse	5′-TGGGAGTAGACAAGGTACAACCC-3′
Il23p19 forward	5′-CAGCAGCTCTCTCGGAAT-3′
Il23p19 reverse	5′-ACAACCATCTTCACACTGGATACG-3′
Il12p40 forward	5′-GAAAGACCCTGACCATCACT-3′
Il12p40 reverse	5′-CCTTCTCTGCAGACAGAGAC-3′
Mpo forward	5′-GCTACCCGCTTCTCCTTCTT-3′
Mpo reverse	5′-TTGCGAATGGTGATGTTGTT-3′
KC forward	5′-TGCACCCAAACCGAAGTCAT-3′
KC reverse	5′-TTGTCAGAAGCCAGCGTTCAC-3′
LIX forward	5′-GGTCCACAGTGCCCTACG-3′
LIX reverse	5′-GCGAGTGCATTCCGCTTA-3′
Lxra forward	5′-TCATGCTTCTGGAGACGT-3′
Lxra reverse	5′-CTCAGCATCATTGAGTTGC-3′
Lxrb forward	5′-CAGCCTTGGTGGTGTCTTCTTGA-3′
Lxrb reverse	5′-CATGGTGTGGTAGGCTGAGGTGTA-3′
Abca1 forward	5′-CGCAAGCATATGCCTCAT-3′
Abca1 reverse	5′-CCCATTACATAACACATGGCT-3′
Apoe forward	5′-AGGATCTACGCAACCGACT-3′
Apoe reverse	5′-CTGCCTTGTACACAGCTA-3′
Pparg forward	5′-TGAATAAAGATGGAGTCCTCATCTCA-3′
Pparg reverse	5′-CTTAGGCTCCATAAAGTCACCAAAG-3′
SREBP-1c forward	5′-AGGCCATCGACTACATCCG-3′
SREBP-1c reverse	5′-TCCATAGACACATCTGTGCCTC-3′
Hmbs forward	5′-GAAACTCTGCTTCGCTGCATT-3′
Hmbs reverse	5′-TGCCCATCTTTCATCACTGTATG-3′

effector cells (47), does not support macrophage-mediated cellular immune defenses triggered by IFN-γ. However, a recent report demonstrated that IL-17 promotes the expression in the lung of chemokines CXCL9, CXCL10, and CXCL11; such expression recruits IFN-γ–producing T cells, which in turn ultimately restrict bacterial growth (48). Such an indirect mechanism may lie at the basis of the LXR-dependent IL-23/IL-17 contribution to protective immunity against *M. tuberculosis*.

Lxra−/− mice have also been shown to be highly susceptible to infection by the intracellular pathogen *Listeria monocytogenes* (32). In the *Listeria* model, or during infection with other bacteria, such

as *Bacillus anthracis*, *Escherichia coli*, and *Salmonella typhimurium*, LXR or LXR/RXR activation antagonized pathogen-induced apoptosis of murine macrophages by promoting the expression of the antiapoptotic factors Spα/AIM and Bcl-X$_L$ and inhibiting proapoptotic gene expression (32, 35). *M. tuberculosis* is also known to manipulate processes linked to cell death, and we also observed LXRα-dependent expression of Spα/AIM mRNA in our model (data not shown). Although we did not detect any difference in expression levels of other pro- or antiapoptotic factors between LXR-deficient mice and their WT counterparts within the limits of our analysis, we cannot exclude the possibility that increased macrophage apoptosis contributes in some way to the susceptible phenotype in *M. tuberculosis*–infected LXR-deficient mice.

Interestingly, the role of LXR in the regulation of neutrophilic inflammation appears to be dependent on the type of pathogen. Thus, Smoak et al. showed that LXR activation impaired, rather than promoted, neutrophil recruitment to the lung in response to the extracellular pathogen *Klebsiella pneumoniae* and rendered mice more susceptible to infection (49). Distinct pathogen-specific molecules acting as pathogen-associated molecular patterns and/or as LXR ligands likely cause the divergent outcomes of LXR activation in these infection models. A report that the fungal metabolite paxilline is a potent LXR agonist supports this proposition (50). In addition, *M. tuberculosis* contains an array of unique lipid components in its outer cell envelope that could act as potential LXR ligands. Mycolic acid, in particular, has been shown to trigger reprogramming of macrophage inflammatory functions along with a strong TLR-2– and TLR-4–independent interference with the lipid metabolism of the cells (16, 51). Alternatively, oxysterols, as naturally occurring, host-derived ligands, may be responsible for LXR activation upon *M. tuberculosis* infection. Increasing evidence points toward an association between the cholesterol metabolism status of the host and the risk of developing pulmonary tuberculosis. Hypocholesterolemia, a condition that reduces the availability of oxysterol LXR agonists, and hence LXR transcriptional activity, has been proposed as a major risk factor for pulmonary tuberculosis (52). Moreover, hypercholesterolemia as a result of high cholesterol diet in mice deficient for ApoE was recently reported to impair immunity to tuberculosis (53). Binding of ApoE to cholesterol-rich plasma lipoproteins such as LDL promotes the uptake of cholesterol from the body fluids through the LDL receptor on tissue macrophages and hepatocytes. It is therefore attractive to speculate that the increased susceptibility of ApoE-deficient mice is the result, at least in part, of a reduced cellular uptake of cholesterol that causes impaired LXR activity analogous to that of LXR-deficient mice. It is noteworthy in this context that mice deficient in LXRs do not show any difference in plasma cholesterol levels, but rather accumulate intracellular cholesterol within peripheral tissue macrophages, and accordingly are not naturally hypercholesterolemic (54, 55).

In conclusion, the present study reveals what we believe to be a novel role for LXRs in the protective immune response against *M. tuberculosis*: modulating both innate and acquired immune responses as well as the lipid metabolism of the host. The dependence of LXR signaling on the IL-23/IL-17 axis represents a function for these nuclear receptors and further supports a contribution of neutrophils and Th17 cells in protective immunity against mycobacterial infections. In order to fully comprehend the relationship between host cholesterol metabolism and the immune defense against *M. tuberculosis*, it is imperative that future studies aim to unravel the mechanism by which LXRs, especially the

inducible LXRα isoform, become activated during infection and regulate Th17 function in the lungs. The ability of synthetic LXR ligands to strengthen host resistance in models of established infection supports further exploration of nuclear receptor signaling pathways as targets for tuberculosis therapeutics.

Methods

Animals. C57BL/6 mice were bred in the animal facilities of the Scientific Institute of Public Health (Brussels, Belgium). Mice were 6–8 weeks of age at the start of experiments. All experiments were reviewed and approved by the ethical committee of the Institute of Public Health–Veterinary and Agrochemical Research Institute (IPH-VAR; Brussels, Belgium). The C57BL/6 *Lxra*−/−, *Lxrb*−/−, *Lxra*−/−*Lxrb*−/−, and matched WT *Lxra*+/+*Lxrb*+/+ mice were generated in our laboratory as previously described (54).

M. tuberculosis infection experiments. Luminescent *M. tuberculosis* H37Rv was grown as a surface pellicle on synthetic Sauton medium as described previously (55). Bacteria were harvested after 2 weeks, and aliquots were stored frozen at –70°C until use. This strain is transformed with pSMT1 plasmid encoding a bacterial luciferase under the control of the constitutive mycobacterial hsp60 promoter (56). Bacterial multiplication was quantified using a bioluminescence assay (for the determination of RLU) in a Turner Designs 20/20 luminometer with 1% n-decanal in ethanol as substrate. We have previously shown that RLU counting in a luminescence assay is a quick and accurate alternative to labor-intensive CFU enumeration on agar plates (55). Unless indicated otherwise, mice were instilled with 5×10^3 mRLU luminescent *M. tuberculosis* H37Rv i.t., corresponding to approximately 10^4 CFU. In some instances, mice were treated with 50 μg of the LXR agonist TO901317 (Sigma-Aldrich), administered i.p. 3 times per week, in either a prophylactic or a therapeutic approach. The agonist solvent (0.1% DMSO/PBS) was used as a control.

Isolation of cell populations from airway lumen and lung tissue. Mice were sacrificed by i.p. injection of 0.5 ml avertin (2.5% w/v in PBS), the trachea was cannulated, and BAL was performed 3 times with 1 ml ice-cold HBSS (Invitrogen) supplemented with 0.05 mM EDTA. The 3 BAL fluid aliquots of each animal were pooled, the cells were pooled by treatment group, and the CD11c+ cell fraction was isolated using CELLection Biotin Binder Kit according to the manufacturer's protocol (Dynal AS, Invitrogen). CD4+ T cells were isolated with the same procedure from homogenized lung tissue samples. Single-cell suspensions of lung tissue were prepared by digestion of minced tissue with RPMI 1640 medium supplemented with 2.4 mg/ml collagenase (Sigma-Aldrich) and 1 mg/ml DNaseI (Roche) for 30 min at 37°C. The digest was passed through a 70-μm cell strainer, and erythrocytes were lysed with NH₄Cl-Tris buffer.

RT-qPCR. RNA was extracted using a commercially available RNeasy kit according to the manufacturer's instructions (Qiagen). cDNA was synthesized using a TaqMan Reverse Transcription Reagent kit (Roche). RT-qPCR was performed on an ABI Prism 7700 Sequence Detector (Applied Biosystems) using a qPCR Core Kit for Sybr Green I (Eurogentec). Each RT-qPCR amplification was performed in triplicate under the following conditions: 50°C for 2 minutes and 95°C for 10 minutes, followed by 40 cycles at 95°C for 15 seconds and 60°C for 1 minute. The forward and reverse primers used are shown in Table 1. Hydroxymethylbilane synthase mRNA was used as reference housekeeping gene for normalization. The

level of target mRNA, relative to the mean of the reference housekeeping gene, was calculated as previously described (51).

Assessment of leukocyte distribution in BAL fluid. Mice were sacrificed by i.p. injection of 0.5 ml avertin (2.5% w/v in PBS), the trachea was cannulated, and BAL was performed. The total volume and cell number recovered from the BAL were recorded. Cytospins were prepared from each sample, fixed, and stained with May-Grünwald/Giemsa (Sigma-Aldrich). Cells were classified as mononuclear cells, neutrophils, eosinophils, and lymphocytes using standard morphological criteria. At least 200 cells were counted per cytospin preparation, and the absolute number of cells for each cell type was calculated.

Histological analysis. Lungs were excised, fixed in 4% paraformaldehyde, and embedded in paraffin. Sections (2.5 μm thick) from all lobes were stained with H&E according to standard histological procedures. To score lung inflammation and damage, the entire lung section was analyzed with respect to granuloma formation, alveolitis, and perivascular and peribronchial inflammation. Each parameter was graded on a 0–5 scale as follows: 0, absent; 1, mild; 2, moderate; 3, extensive; 4, severe; 5, very severe. As 5–7 tissue sections per mouse were scored, inflammation scores could be expressed as a mean value per animal and could be compared between groups. Acid fast staining of the mycobacteria was performed according to the manufacturer's instructions and counterstained with methylene blue included in the kit (Thermo Shandon). The bacilli were located by visual inspection of 20 random fields as well as by analysis of 20 fields at specific locations of the primary granuloma. Oil Red O staining was performed as previously described (57) and quantified by microscopic examination of 20 random fields. Macrophages were considered to be foam cells if they contained 10 or more Oil Red–positive lipid droplets.

Statistics. Values are expressed as mean ± SD unless otherwise indicated. The Kruskal-Wallis test was used first to ascertain that significant variance existed among the groups studied. The Mann-Whitney U test was then used to test statistical significance of the differences between 2 groups. A P value less than 0.05 was considered statistically significant.

Address correspondence to: Kris Huygen, Laboratory of Mycobacterial Immunology, Scientific Institute of Public Health, 642 Engelandstraat, B1180 Brussels, Belgium. Phone: 32-2-373-33-71; Fax: 32-2-373-33-67; E-mail: Kris.Huygen@iph.fgov.be.

Jan-Åke Gustafsson's present address is: Department of Biology and Biochemistry, University of Houston, Houston, Texas, USA.

1. WHO. 2005. Tuberculosis [fact sheet]. Revised March 2007. http://www.who.int/mediacentre/factsheets/fs104/en.
2. Manabe, Y.C., and Bishai, W.R. 2000. Latent Mycobacterium tuberculosis-persistence, patience, and winning by waiting. *Nat. Med.* **6**:1327–1329.
3. Rengarajan, J., Bloom, B.R., and Rubin, E.J. 2005. Genome-wide requirements for Mycobacterium

tuberculosis adaptation and survival in macrophages. *Proc. Natl. Acad. Sci. U. S. A.* **102**:8327–8332.
4. Schnappinger, D., et al. 2003. Transcriptional adaptation of *Mycobacterium tuberculosis* within macrophages: insights into the phagosomal environment. *J. Exp. Med.* **198**:693–704.
5. Voskuil, M.I., et al. 2003. Inhibition of respiration by nitric oxide induces a Mycobacterium tubercu-

losis dormancy program. *J. Exp. Med.* **198**:705–713.
6. Bloch, H., and Segal, W. 1956. Biochemical differentiation of Mycobacterium tuberculosis grown in vivo and in vitro. *J. Bacteriol.* **72**:132–141.
7. Wheeler, P.R., and Ratledge, C. 1988. Use of carbon sources for lipid biosynthesis in Mycobacterium leprae: a comparison with other mycobacteria. *J. Gen. Microbiol.* **134**:2111–2121.

8. Ehrt, S., and Schnappinger, D. 2007. Mycobacterium tuberculosis virulence: lipids inside and out. *Nat. Med.* **13**:284–285.

9. McKinney, J.D., et al. 2000. Persistence of Mycobacterium tuberculosis in macrophages and mice requires the glyoxylate shunt enzyme isocitrate lyase. *Nature.* **406**:735–738.

10. Kendall, S.L., et al. 2007. A highly conserved transcriptional repressor controls a large regulon involved in lipid degradation in Mycobacterium smegmatis and Mycobacterium tuberculosis. *Mol. Microbiol.* **65**:684–699.

11. Van der Geize, R., et al. 2007. A gene cluster encoding cholesterol catabolism in a soil actinomycete provides insight into Mycobacterium tuberculosis survival in macrophages. *Proc. Natl. Acad. Sci. U. S. A.* **104**:1947–1952.

12. Pandey, A.K., and Sassetti, C.M. 2008. Mycobacterial persistence requires the utilization of host cholesterol. *Proc. Natl. Acad. Sci. U. S. A.* **105**:4376–4380.

13. Gatfield, J., and Pieters, J. 2000. Essential role for cholesterol in entry of mycobacteria into macrophages. *Science.* **288**:1647–1650.

14. Peyron, P., Bordier, C., N'Diaye, E.N., and Maridonneau-Parini, I. 2000. Nonopsonic phagocytosis of Mycobacterium kansasii by human neutrophils depends on cholesterol and is mediated by CR3 associated with glycosylphosphatidylinositol-anchored proteins. *J. Immunol.* **165**:5186–5191.

15. de Chastellier, C., and Thilo, L. 2006. Cholesterol depletion in Mycobacterium avium-infected macrophages overcomes the block in phagosome maturation and leads to the reversible sequestration of viable mycobacteria in phagolysosome-derived autophagic vacuoles. *Cell. Microbiol.* **8**:242–256.

16. Korf, J., Stoltz, A., Verschoor, J., De Baetselier, P., and Grooten, J. 2005. The Mycobacterium tuberculosis cell wall component mycolic acid elicits pathogen-associated host innate immune responses. *Eur. J. Immunol.* **35**:890–900.

17. Ordway, D., Henao-Tamayo, M., Orme, I.M., and Gonzalez-Juarrero, M. 2005. Foamy macrophages within lung granulomas of mice infected with Mycobacterium tuberculosis express molecules characteristic of dendritic cells and antiapoptotic markers of the TNF receptor-associated factor family. *J. Immunol.* **175**:3873–3881.

18. Hunter, R.L., Jagannath, C., and Actor, J.K. 2007. Pathology of postprimary tuberculosis in humans and mice: contradiction of long-held beliefs. *Tuberculosis (Edinb.).* **87**:267–278.

19. Peyron, P., et al. 2008. Foamy macrophages from tuberculous patients' granulomas constitute a nutrient-rich reservoir for M. tuberculosis persistence. *PLoS Pathog.* **4**:e1000204.

20. Ricote, M., Valledor, A.F., and Glass, C.K. 2004. Decoding transcriptional programs regulated by PPARs and LXRs in the macrophage: effects on lipid homeostasis, inflammation, and atherosclerosis. *Arterioscler. Thromb. Vasc. Biol.* **24**:230–239.

21. Valledor, A.F. 2005. The innate immune response under the control of the LXR pathway. *Immunobiology.* **210**:127–132.

22. Mitro, N., et al. 2007. The nuclear receptor LXR is a glucose sensor. *Nature.* **445**:219–223.

23. Janowski, B.A., Willy, P.J., Devi, T.R., Falck, J.R., and Mangelsdorf, D.J. 1996. An oxysterol signalling pathway mediated by the nuclear receptor LXR alpha. *Nature.* **383**:728–731.

24. Lehmann, J.M., et al. 1997. Activation of the nuclear receptor LXR by oxysterols defines a new hormone response pathway. *J. Biol. Chem.* **272**:3137–3140.

25. Fu, X., et al. 2001. 27-hydroxycholesterol is an endogenous ligand for liver X receptor in cholesterol-loaded cells. *J. Biol. Chem.* **276**:38378–38387.

26. Repa, J.J., and Mangelsdorf, D.J. 2000. The role of orphan nuclear receptors in the regulation of cholesterol homeostasis. *Annu. Rev. Cell Dev. Biol.* **16**:459–481.

27. Chawla, A., Repa, J.J., Evans, R.M., and Mangelsdorf, D.J. 2001. Nuclear receptors and lipid physiology: opening the X-files. *Science.* **294**:1866–1870.

28. Repa, J.J., et al. 2000. Regulation of absorption and ABC1-mediated efflux of cholesterol by RXR heterodimers. *Science.* **289**:1524–1529.

29. Venkateswaran, A., et al. 2000. Control of cellular cholesterol efflux by the nuclear oxysterol receptor LXR alpha. *Proc. Natl. Acad. Sci. U. S. A.* **97**:12097–12102.

30. Castrillo, A., and Tontonoz, P. 2004. Nuclear receptors in macrophage biology: at the crossroads of lipid metabolism and inflammation. *Annu. Rev. Cell Dev. Biol.* **20**:455–480.

31. Joseph, S.B., Castrillo, A., Laffitte, B.A., Mangelsdorf, D.J., and Tontonoz, P. 2003. Reciprocal regulation of inflammation and lipid metabolism by liver X receptors. *Nat. Med.* **9**:213–219.

32. Joseph, S.B., et al. 2004. LXR-dependent gene expression is important for macrophage survival and the innate immune response. *Cell.* **119**:299–309.

33. Castrillo, A., et al. 2003. Crosstalk between LXR and toll-like receptor signaling mediates bacterial and viral antagonism of cholesterol metabolism. *Mol. Cell.* **12**:805–816.

34. Fontaine, C., et al. 2007. Liver X receptor activation potentiates the lipopolysaccharide response in human macrophages. *Circ. Res.* **101**:40–49.

35. Valledor, A.F., et al. 2004. Activation of liver X receptors and retinoid X receptors prevents bacterial-induced macrophage apoptosis. *Proc. Natl. Acad. Sci. U. S. A.* **101**:17813–17818.

36. Collins, J.L. 2004. Therapeutic opportunities for liver X receptor modulators. *Curr. Opin. Drug Discov. Devel.* **7**:692–702.

37. Vermaelen, K., and Pauwels, R. 2004. Accurate and simple discrimination of mouse pulmonary dendritic cell and macrophage populations by flow cytometry: methodology and new insights. *Cytometry A.* **61**:170–177.

38. Rausch, P.G., Pryzwansky, K.B., Spitznagel, J.K., and Herion, J.C. 1978. Immunocytochemical identification of abnormal polymorphonuclear neutrophils in patients with leukemia. *Blood Cells.* **4**:369–382.

39. Smith, E., et al. 2007. IL-23 is required for neutrophil homeostasis in normal and neutrophilic mice. *J. Immunol.* **179**:8274–8279.

40. Goerdt, S., and Orfanos, C.E. 1999. Other functions, other genes: alternative activation of antigen-presenting cells. *Immunity.* **10**:137–142.

41. Gordon, S. 2003. Alternative activation of macrophages. *Nat. Rev. Immunol.* **3**:23–35.

42. Nair, M.G., Cochrane, D.W., and Allen, J.E. 2003. Macrophages in chronic type 2 inflammation have a novel phenotype characterized by the abundant expression of Ym1 and Fizz1 that can be partly replicated in vitro. *Immunol. Lett.* **85**:173–180.

43. Raes, G., et al. 2002. Differential expression of FIZZ1 and Ym1 in alternatively versus classically activated macrophages. *J. Leukoc. Biol.* **71**:597–602.

44. Kahnert, A., et al. 2006. Alternative activation deprives macrophages of a coordinated defense program to Mycobacterium tuberculosis. *Eur. J. Immunol.* **36**:631–647.

45. Pedrosa, J., et al. 2000. Neutrophils play a protective nonphagocytic role in systemic Mycobacterium tuberculosis infection of mice. *Infect. Immun.* **68**:577–583.

46. Seiler, P., et al. 2000. Rapid neutrophil response controls fast-replicating intracellular bacteria but not slow-replicating Mycobacterium tuberculosis. *J. Infect. Dis.* **181**:671–680.

47. Laan, M., et al. 1999. Neutrophil recruitment by human IL-17 via C-X-C chemokine release in the airways. *J. Immunol.* **162**:2347–2352.

48. Khader, S.A., et al. 2007. IL-23 and IL-17 in the establishment of protective pulmonary CD4+ T cell responses after vaccination and during Mycobacterium tuberculosis challenge. *Nat. Immunol.* **8**:369–377.

49. Smoak, K., et al. 2008. Effects of liver X receptor agonist treatment on pulmonary inflammation and host defense. *J. Immunol.* **180**:3305–3312.

50. Bramlett, K.S., et al. 2003. A natural product ligand of the oxysterol receptor, liver X receptor. *J. Pharmacol. Exp. Ther.* **307**:291–296.

51. Korf, J.E., et al. 2006. Macrophage reprogramming by mycolic acid promotes a tolerogenic response in experimental asthma. *Am. J. Respir. Crit. Care Med.* **174**:152–160.

52. Perez-Guzman, C., and Vargas, M.H. 2006. Hypocholesterolemia: a major risk factor for developing pulmonary tuberculosis? *Med. Hypotheses.* **66**:1227–1230.

53. Martens, G.W., et al. 2008. Hypercholesterolemia impairs immunity to tuberculosis. *Infect. Immun.* **76**:3464–3472.

54. Alberti, S., et al. 2001. Hepatic cholesterol metabolism and resistance to dietary cholesterol in LXR-beta-deficient mice. *J. Clin. Invest.* **107**:565–573.

55. Tanghe, A., et al. 2001. Improved immunogenicity and protective efficacy of a tuberculosis DNA vaccine encoding Ag85 by protein boosting. *Infect. Immun.* **69**:3041–3047.

56. Snewin, V.A., et al. 1999. Assessment of immunity to mycobacterial infection with luciferase reporter constructs. *Infect. Immun.* **67**:4586–4593.

57. Tracy, R.E., and Walia, P. 2004. Lipid fixation for fat staining in paraffin sections applied to lesions of atherosclerosis. *Virchows Arch.* **445**:22–26.